IEEE Open Journal of
Power Electronics

Received 16 April 2024; revised 27 May 2024; accepted 3 June 2024. Date of publication 7 June 2024;
date of current version 18 June 2024. The review of this article was arranged by Associate Editor Giovanni De Carne.

Digital Object Identifier 10.1109/OJPEL.2024.3411110

A Review of Voltage-Clamping Methods for Solid-State Circuit Breakers

GIOELE GREGIS [1], LUIGI PIEGARI [1] (Senior Member, IEEE), LUCA RACITI [2], AND THOMAS MASPER [2]

[1]Department of Electronics, Information and Bioengineering, Politecnico di Milano, 20133 Milano, Italy
[2]Smart Power division of ABB, 24123 Bergamo, Italy

(CORRESPONDING AUTHOR: GIOELE GREGIS (e-mail: gioele.gregis@polimi.it)

ABSTRACT In recent years, the interest in DC systems has increased dramatically because of some key advantages, in terms of efficiency and reliability, that this technology can offer compared to AC systems in applications such as shipboard distribution, more electric aircrafts, DC microgrids, battery protection, and photovoltaics. In this context, DC circuit breakers based on power semiconductors, the so-called solid-state circuit breakers, are becoming a popular choice because of their fast intervention speed, which is typically on the order of microseconds. Unfortunately, power electronics are vulnerable to "breakdown", which is a dangerous operating condition triggered by overvoltages. During current interruption, the energy stored in the inductive elements of the system must be dissipated, and this typically creates a very high voltage spike on the interrupting component, which is the breaker pole. This phenomenon, if not controlled, could lead to the premature failure of the semiconductor inside the solid-state circuit breaker. For this reason, suitable techniques aimed to control the voltage gradient and overshoot during interruption have been presented in the literature. This paper analyzes and compares the performances of the voltage-clamping solutions presented in the technical literature, which range from simple passive devices to more advanced solutions.

INDEX TERMS DC power systems, snubbers, DC circuit breakers, SSCBs.

I. INTRODUCTION

DC systems have attracted much interest in recent years because they offer an intrinsic advantage in terms of efficiency and reliability compared to AC systems [1], [2]. The applications where these aspects have become relevant include shipboard distribution systems [3], [4], [5], [6], datacenters [7], [8], and more electric aircraft (MEA) [9], [10]. However, because of increased environmental concerns, more and more DC systems are starting to appear as a result of the diffusion of photovoltaic (PV) panels, battery energy storage systems (BESSs), and charging stations for electric vehicles. These elements typically form a DC microgrid [11].

DC distribution grids are commonly realized using either a voltage source converter (VSC) connected to an AC grid or DC sources such as batteries and PV panels, typically coupled with DC–DC converters used for voltage and power regulation. In both cases, a large capacitor is installed on the DC microgrid side of these conversion stages to smooth the voltage oscillations. Moreover, all the loads connected to the DC grid, such as variable frequency drives, are typically interfaced with the same kind of converter. The high number of distributed capacitances in the network is the reason why, in the case of a short circuit on the DC line, the current can reach very high values in a short period of time [12]. In addition to the electrothermal and electrodynamic problems that a high current poses for the conductors, if the fault is not interrupted fast enough, the voltage on the bus will decrease dramatically as a result of the discharge of the capacitors. This condition would put the DC system out of service because the connected converters are no longer capable of regulation [13].

DC circuit breakers (DCCBs) are critical components [14]. Traditional mechanical circuit breakers (CBs) in AC systems exploit the natural zero crossing of the current to break the circuit without (or with minimal) arc formation. In DC, there is no natural zero crossing of the current and the CB must break the arc. This causes a long interruption time and high dissipated energy. In the case of a fault, to protect the DC system, it would be beneficial to interrupt the current and isolate the fault as fast as possible. Traditional DCCBs are

not fast enough for this operation. Moreover, the hybrid DC-CBs proposed in the literature are too slow in many cases. Therefore, solid-state circuit breakers (SSCBs) are the most commonly proposed solution for very fast protection of DC microgrids.

However, the fast current cutoff of a SSCB creates a huge overvoltage on the semiconductor component because of the inductance present in the system. Semiconductor devices are generally susceptible to breakdown events triggered by overvoltages. Therefore, an unclamped current interruption would produce high stresses on the breaker components, which would eventually lead to the early failure of the device. Part 6 of *"Power Electronics: Converters, Applications and Design"* [15] presents more details about the breakdown phenomenon in power semiconductor devices.

Electromechanical circuit breakers dissipate the inductive energy in the air using an arc chamber. However, this is not present in SSCBs because the current is interrupted by a semiconductor device with no moving parts. Thus, several voltage clamping techniques have been presented in the literature for controlling the voltage overshoot and time derivative of the voltage (*dv/dt*) across the semiconductor component. These range from the classic resistor-capacitor-diode (RCD) snubber and metal oxide varistors (MOVs) to more elaborated structures.

This paper analyzes the methods available in the literature for controlling the overvoltage across an SSCB, as well as dissipating the inductive energy in the line.

Other papers have analyzed the snubber circuits used for SSCBs. In particular, Rodrigues et al. presented in [12] a general overview of clamping techniques from the literature up to 2020, while the authors of [16] experimentally tested the behaviors of some of those solutions. In [17] Giannakis et al. compared the performances of just three configurations, namely the MOV, the RCD, and the two together. In [18] Zhao et al. investigated the limitations of MOVs and MOV+RCD snubbers in terms of the intervention speed and impact of the snubber on the gate voltage, while the authors of paper [19] focused on a comparison of MOV and MOV+RC snubbers applied to integrated gate-commutated thyristor (IGCT)-based SSCBs.

Here, a direct comparison of several snubbers is presented, as well as analyses of the most novel solutions proposed in the literature after 2020. Considering the standard proposal for DC grids [13], some requirements for designing snubbers for SSCBs are also introduced and some relevant challenges are presented.

The analysis starts with the well-known passive snubbers such as an RCD snubber or MOV and continues with more advanced topologies and devices using controlled switches. Finally, the novel clamping solutions proposed in recent years, such as the "electronic MOV", are introduced and discussed.

In the conclusion, all the solutions presented are compared and some guidelines to choose the best clamping circuit for different applications are given.

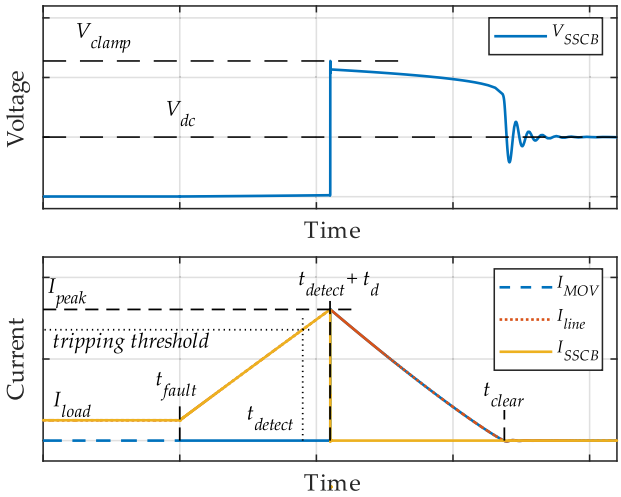

FIGURE 1. SSCB equipped with MOV: Typical waveforms during fault current interruption.

II. COMPARISON CRITERIA AND CHALLENGES

In order to classify and compare the different snubbers presented, the following comparison criteria will be adopted:

- minimum number of components used for a bidirectional snubber;
- energy handling capability;
- current handling capability;
- switch voltage utilization ratio;
- turn-off oscillation damping.

These criteria, apart from the first one for obvious reasons, will be classified on a scale from 1 to 5 (also color coded from red to dark green) to qualitatively address the relative performance of each snubber, where 1 (red) indicates the worst performance and 5 (dark green) indicates the best performance.

Choosing the proper snubber circuit for a given application is crucial for the correct operation of a breaker. The network of an onboard marine DC system is quite different from an industrial one. In particular, marine plants are typically custom made. Thus, the SSCBs and their snubbers can be fine-tuned to the specific operating conditions, while the devices used in industrial applications are typically bought off the shelf. Therefore, the SSCBs have to adapt to a broad range of working conditions.

An example of the interruption waveform for a SSCB is shown in Fig. 1. In this example, an MOV is used as the snubber circuit. The typical SSCB current interruption process occurs in the following way: the breaker is carrying load current I_{load} before a fault occurs at time t_{fault}. The current then starts rising with a slope that depends on the system inductance. Once the tripping threshold is reached at t_{detect}, the SSCB commands an opening and after intrinsic delay t_{d}, the current reaches I_{peak} and stops increasing. At that point, the SSCB has effectively opened and current commutates to the snubber circuit. At the same time, the voltage across

the SSCB increases to V_{clamp}. The overvoltage above V_{dc} allows the current to decrease, and finally the fault is cleared at time t_{clear}. It should be noted that this time depends on the system inductance, as well as the peak current interrupted and overvoltage magnitude.

From this discussion, it is clear that the choice of snubber circuit and its design parameters, such as the clamping voltage and maximum absorbable energy, severely impact the current interruption capability of the breaker, as highlighted by Ravi et al. in [20].

The main requirements when designing a snubber circuit applied to an SSCB are summarized in the following points:

- clamping voltage should stay constant at the desired value;
- *dv/dt* should be controlled during turn off to avoid excessive losses in semiconductor switches and current flowing inside parasitic capacitances;
- leakage current should be very low;
- it should work with bidirectional current flow;
- it should not be affected by a change in the polarity of the DC bus.

While the last two points are not strictly required for functionality, they bring value to the solution, allowing it to be used in a larger number of applications.

Moreover, to correctly address the snubber design process, the variables that define the boundaries of the operating conditions should be identified beforehand. These are nominal bus voltage V_{dc}, prospective peak turn-off current I_{peak}, the breakdown voltage of the semiconductor used, and an estimation of the system and fault inductance.

It is now worth highlighting some critical aspects and challenges that must be considered during the design process of a snubber for an SSCB.

First, time delay t_d, together with the fault inductance and bus voltage, will determine the actual peak turn-off current. This time is influenced by many factors such as the gate driving resistors, protection algorithm, and current sensor bandwidth. This becomes particularly important when the network has been designed with a very low inductance.

Another challenge encountered during voltage clamping design is finding a component capable of transitioning from the leakage mode to fully clamping mode in a narrow voltage band. Indeed, building a device that blocks V_{dc} with a reasonable leakage current and clamps the voltage below the breakdown voltage of semiconductor devices at the peak fault current is not trivial, especially with the goal of reducing semiconductor oversizing as much as possible.

Additionally, overcurrent faults may belong to completely different categories: slow and high energy faults, or fast and low energy faults. Handling both of these with the same snubber circuit may be cumbersome, especially when all the previous points are taken into account.

Finally, in a case where several circuits are connected to the same point, the source-side inductance may induce a dangerous overvoltage on neighboring devices once one circuit is tripped. Thus, this aspect should be addressed during design. In case any problem arises, additional components to manage the source inductance should be included in the snubber circuit.

III. BASIC CONCEPTS FOR VOLTAGE CLAMPING

Snubber circuits, by definition, are designed and employed to control the rate of change of the current/voltage or to suppress current/voltage overshoots across critical elements of the circuit. Typically, the field of application has been inside power converters to protect semiconductor switches from inductance-induced overvoltages during commutation; some examples of the applications and design guidelines can be found in [21].

In power converters, the main goal during the design phase of a snubber is to minimize power losses because switching events are frequent. For this reason, the design guidelines presented in the literature aim to minimize the presence of dissipative components. As a further evolution, this idea leads to the so-called non-dissipative or regenerative snubbers, which store and release energy from/to the load between switching events.

In an SSCB application, snubbers, which are also called voltage clamps, are required to suppress the overvoltages that appear across the semiconductor switches during turn off due to the inductance present in the commutation path. The consecutive turn-on and turn-off events are far less frequent with respect to a power converter. Therefore, the efficiency of the snubber is not the main concern. In fact, for SSCBs, the snubbers are typically required to absorb much more energy to keep the overvoltage under control. For this reason, the approach to design a snubber for an SSCB is fundamentally different from the approach adopted to design a power converter snubber. It should also be noted that there is a fundamental relationship between the clamping voltage values, energy dissipated inside the snubber elements, and fault isolation speed. As shown in [22], higher clamping voltages lead to lower values for the current interruption time and energy dissipated, as shown in (1).

$$W_{clamp} = \left(1 + \frac{V_{dc}}{V_{clamp} - V_{dc}}\right) \frac{1}{2} L I_{peak}^2 \tag{1}$$

It is clear that regarding the fault isolation speed and energy handling capability of a snubber, the design should target a voltage clamp value that is as high as possible, i.e., close to the breakdown limit of the semiconductor components, V_{dss}. In contrast, considering safety, the design should target a lower clamping voltage.

The simplest types of voltage clamping devices presented in the literature are those that use passive components; these devices are directly derived from the well-known snubber topologies typically employed inside power converters. Therefore, early studies on the voltage snubbers applied to SSCBs have already extensively analyzed their properties. These structures are briefly recalled here for completeness. In the literature, there are several papers discussing basic snubbers. Among these, two are of particular interest. In [12], Rodrigues

et al. presented an overall summary of various voltage clamping techniques, commenting on the pros and cons of different choices. Similar results were obtained in [16], where Song et al. tested several types of snubbers in order to experimentally observe the behaviors of different solutions.

Voltage clamps using only linear components are the simplest available; however, they are less effective at suppressing overvoltages and controlling *dv/dt*.

The possible topologies are as follows:

- capacitor (C);
- resistor + capacitor (RC).

While these clamps are simple in terms of the number of components used, they suffer some drawbacks. In particular C snubbers may require an impractically high value of capacitance to absorb the line inductance energy. Moreover, the capacitance discharge current at SSCB turn on may be too high and cause unwanted trips of the breaker. A solution for the latter point is the RC snubber. However, this topology requires a high-power resistor and increases the voltage clamping level as a result of the resistive voltage drop.

In addition, snubbers that employ nonlinear components such as semiconductor devices and/or varistors are capable of achieving a more favorable behavior in terms of the clamping voltage and *dv/dt* control.

In this case, the following topologies are possible:

- resistor + capacitor + diode (RCD);
- metal oxide varistor (MOV);
- transient voltage suppression diode (TVS);
- gas discharge tube (GDT)+dissipation device;
- active clamp;
- any combination of the structures above, e.g., MOV+RC.

A few practical designs considerations can be derived from the analyses of [12] and [16]. The first is general and relates to the range in which the clamping voltage of a real snubber can vary:

$$1.5V_{dc} < V_{clamp} < 2.5V_{dc} < V_{dss} \tag{2}$$

where V_{clamp} is the clamping voltage (typically lower than the semiconductor breakdown voltage if the snubber is across the SSCB), and V_{dc} is the nominal SSCB voltage, i.e., the DC bus voltage. This constraint has been derived experimentally and represents a tradeoff between the fault isolation speed and voltage exploitation of the semiconductor component, favored by high V_{clamp}, and safe clamp voltage level, favored by low V_{clamp}.

Nonetheless, in [16], it was suggested that ratio $V_{\text{clamp}}/V_{\text{dc}}$, which is sometimes called the *switch voltage utilization*, should be considered as a metric to evaluate and compare the performances of different snubber solutions. When choosing a clamping solution, a value close to one should be targeted to achieve a higher voltage exploitation of the semiconductor components, which is the capability to use a higher DC bus voltage for a given semiconductor voltage class. In any case, a negative voltage, either generated through an overvoltage on the commutating SSCB or by other means, is required on the fault/line inductance in order to drive its current to zero.

Fig. 2 shows some examples of how the previously mentioned snubbers are applied to a bidirectional SSCB pole based on metal-oxide-semiconductor field effect transistors (MOSFETs). In addition to these snubbers, which are the most common, Song et al. tested another passive voltage clamp composed of two varistors and an appropriately connected capacitor. This was initially presented in [23] and was later adapted in a MOV+MOV+RC snubber by Zhao et al. in [24]. Fig. 3 shows how these two snubbers are applied to a bidirectional SSCB pole based on MOSFETs.

It should be noted that the behavior of the snubber shown in Fig. 3(a) is similar to that of Fig. 2(e). However, replacing the resistor with a MOV increases the damping of the LC oscillations at the end of turn off (the behavior represented as an example in Fig. 1 around t_{clear}).

In the following paragraphs, the most common topologies, as well as novel ones, will be shown and compared in detail.

A. RCD SNUBBER AND ITS VARIATIONS

RCD snubbers are commonly used for SSCBs because they have been thoroughly analyzed for power converter applications. Papers [25] and [26] studied the application of RCD snubbers to SSCBs, considering two different topologies. The first was the well-known RCD snubber already presented in Fig. 2(c) and shown again in Fig. 4 for convenience. This topology is also called the *"charge-discharge type"* because of the dynamic of the capacitor during operation.

When the SSCB is open, the capacitors charge to a certain voltage (V_{dc} at the steady state); then when the SSCB closes, the capacitors discharge through it, with the discharge current limited by the resistors. When the SSCB needs to be tripped, the current commutates through the capacitor and diode path, and the inductive energy is absorbed inside the capacitor, which limits the voltage overshoot. This charging and discharging behavior, which is also present in RC snubbers, reduces the fault isolation speed because when the SSCB turns off, the current commutates to the snubber and keeps increasing until the capacitor voltage has at least reached the DC bus voltage. The excessive energy is then dissipated inside the resistor with oscillations until the voltage returns to the DC bus level.

The second type of RCD snubber analyzed in [25] and [26] is called "*discharge-suppressing type I*" and is represented in Fig. 5. In this case, the capacitor is charged at the DC bus voltage and does not discharge when the switch closes. When the SSCB opens as the result of a trip, the current stop increasing immediately because the capacitor was already charged to the DC bus voltage; this is a great advantage compared to the *charge-discharge type*. In this case also, the excessive energy is dissipated inside the resistor, although with less oscillations because the diode is blocking the path to the fault inductance.

The structure shown in Fig. 5 is not bidirectional and requires some adjustment. Therefore, the authors in [25] proposed the solution reported in Fig. 6, along with some design

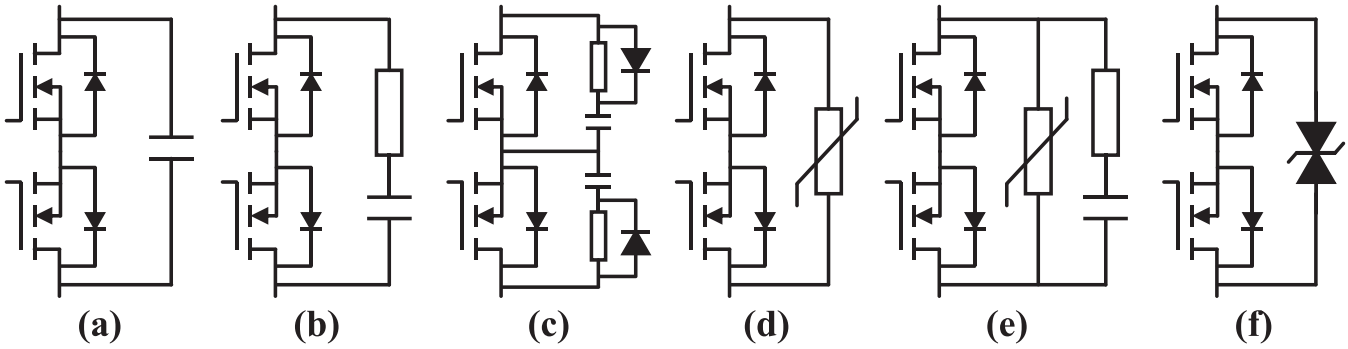

FIGURE 2. Basic snubber topologies applied to the MOSFET bidirectional SSCB analyzed in [16]: (a) C, (b) RC, (c) RCD, (d) MOV, (e) MOV+RC, and (f) TVS.

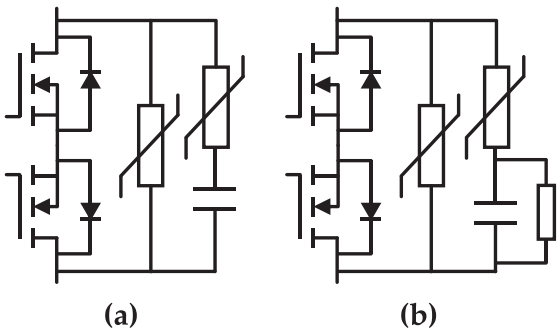

FIGURE 3. Snubber topologies applied to a MOSFET bidirectional SSCB: (a) MOV+MOV+C [23] and (b) MOV+MOV+RC [24].

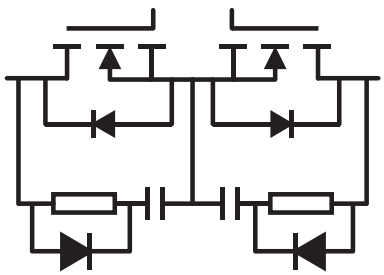

FIGURE 4. Example of a bidirectional *charge-discharge type* RCD snubber [25], [26].

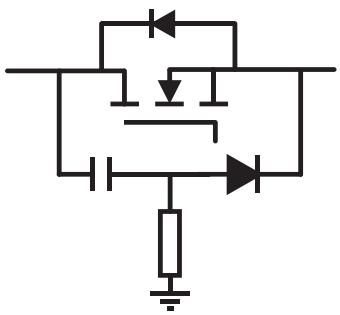

FIGURE 5. Example of a *discharge-suppressing type I* RCD snubber [25], [26].

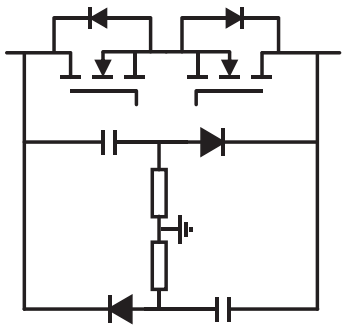

FIGURE 6. Example of a bidirectional *discharge-suppressing type I* RCD snubber [25].

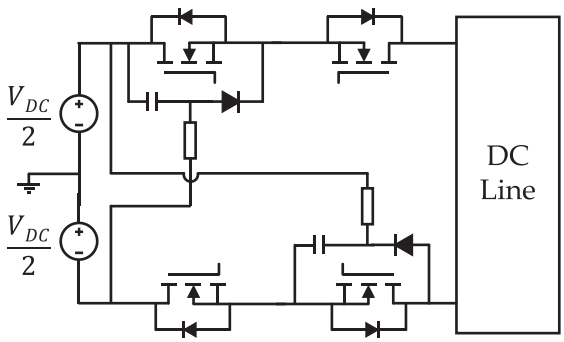

FIGURE 7. Example of a *discharge-suppressing type II* RCD snubber [26].

criteria to choose the values of the capacitor and resistors based on the maximum desired overvoltage and maximum breakable current.

The fact that a resistor is required for power dissipation creates some criticalities during design, which is why Wang et al. in [27] proposed the same structure as that shown in Fig. 5. However, they used an MOV instead of a resistor. Although the working principle is the same, it eliminates the need for a high-power-rated component.

The work presented in [26] introduced another topology, called "*discharge-suppressing type II*" (Fig. 7), and compared its performances to those of the RCD topologies already analyzed. This topology is possible only when a bipolar

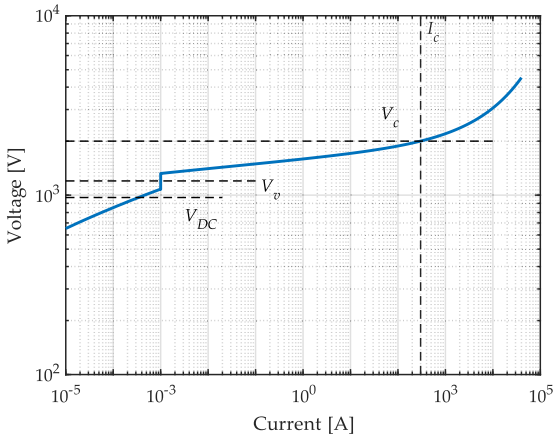

FIGURE 8. Example of MOV characteristics (TDK B72240L0751K102) [28].

line is used and the working principle is the same as that of *discharge-suppressing type I*. In a bipolar line, the supply midpoint is typically grounded, and a negative voltage line is available. Therefore, the snubber resistor could be connected to the ground, which would again form a *discharge-suppressing type I* topology, where the snubber capacitors get charged to $\pm V_{dc}/2$, or to the opposite line, in which case the capacitors are charged to $\pm V_{dc}$. In both cases, a positive value is obtained for the snubber capacitor related to the SSCB pole connected in series with the positive line, while a negative value is obtained for the snubber capacitor related to the SSCB pole connected in series with the negative line.

It is important to notice that with the *discharge-suppressing type II* RCD snubber there is a connection, through some passive components, between the positive and negative poles of the DC line. Thus, this architecture increases the leakage current drawn from the supply. Moreover, some care must be taken when designing the creepage and clearance distances because this connection can create a critical discharge path.

B. METAL OXIDE VARISTORS

Metal oxide varistors are nonlinear resistors made of a semiconductor material such as zinc oxide and are typically used to suppress overvoltages on power lines. Their *I–V* characteristics can be divided in two parts. When the applied voltage is below a given threshold, which is usually defined as the voltage that forces 1 mA through the MOV, the device exhibits a high impedance; above that value, the current flowing increases rapidly, while the voltage stays relatively constant. An example of MOV characteristics (TDK B72240L0751K102) [28] is shown in Fig. 8, and its main parameters, taken from [29], are reported in Table 1.

MOVs can be implemented in a standalone configuration to suppress overvoltages across SSCBs, as seen in Fig. 2(d). However, their performances may vary depending on the peak current and *di/dt* being interrupted. In the presence of fast current slopes, the peak clamping voltage may be much higher than expected as a result of the parasitic inductance of the device and some processes related to the varistor material.

TABLE 1. Main Parameters of MOV B72240L0751K102 [29]

Parameter	Value	Description
V_{RMS}	750 V	Maximum operating AC RMS voltage
V_{DC}	970 V	Maximum operating DC voltage
V_v	1200 V	Maximum voltage at 1mA current
W_{max}	1200 J	Rated energy absorption capability
P_{max}	1.4 W	Maximum continuous dissipated power
V_c	2000 V	Clamping voltage at I_c
I_c	300 A	Current flowing at V_c

This is the so-called *"steep front effect"* of an MOV and was initially analyzed in [30], [31]. Moreover, the characteristics of MOVs degrade with repetitive surge events. Therefore this aging must be considered during their design. Indeed, several studies have analyzed how an MOV degrade and how to predict its lifetime [32], [33], [34], [35]. Nonetheless, to achieve the required characteristics in terms of V_{clamp} and peak-current interruption, more MOVs can be placed in series and/or parallel. However, this may introduce the problem of unbalanced voltage and/or current sharing among the MOVs due to the tolerances and non-linearities of the device. Some analyses on the serialization MOVs were carried out in [36]. The target was a hybrid SSCB rated for HVDC. Therefore, many semiconductor switches for the SSCB, as well as MOVs, were used in series to achieve the required voltage level. The paper showed that a RC circuit in parallel with every MOV could be used to achieve a dynamic voltage balance and suppress the first voltage spike due to the steep front effect of the MOV.

Papers [37], [38], [39] focused on the impact of the stray inductance of an MOV on the peak V_{clamp}. The solution proposed by the authors adopted an additional MOV rated for lower energy but higher voltage in order to have a physically smaller component that could be mounted closer to the SSCB. In this way, the parasitic loop inductance was lower, and the initial voltage spike was reduced; then, current was commutated to the main MOV rated for a lower voltage but higher energy, and the line energy was dissipated. In this way, the clamping voltage control and energy absorption function were separated into two different devices, which could be tuned accordingly.

In paper [40], an MOV and a *discharge-suppressing type I* RCD snubber were compared. The results showed that the MOV clamping voltage was higher than that of the RCD snubber for a given current, and thus the clearing times were shorter. Moreover, the MOV exhibited some ringing during clamping as a result of its parasitic capacitance oscillating with the fault/line inductance. Nonetheless, the MOV solution is cheaper than the RCD snubber because it uses fewer components. Another use of an MOV is in combination with other types of snubbers; paper [41] analyzed the design procedure

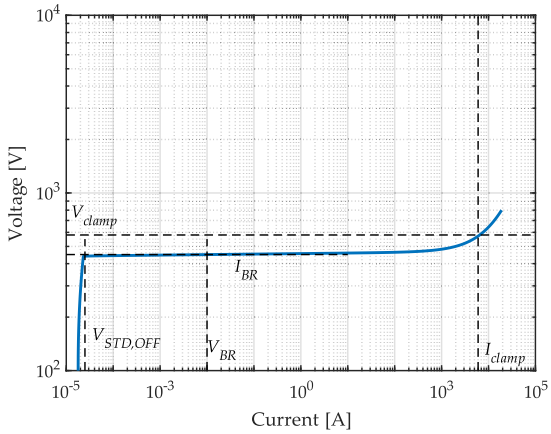

FIGURE 9. Example of TVS V–I characteristics (rated for 430 V/6 kA) [42].

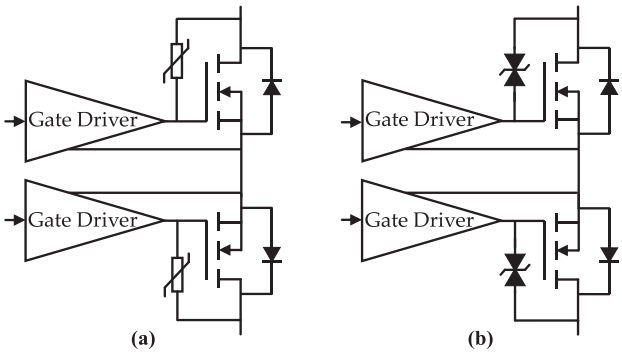

FIGURE 10. Examples of active clamp implementation: (a) MOV active clamp and (b) TVS active clamp [45], [46], [47].

of an MOV+RCD snubber to achieve a fast, but smooth, transient response.

C. TRANSIENT VOLTAGE SUPPRESSION DIODE

Transient voltage suppression diodes (TVSs) are a special kind of diodes made of silicon that exploit the avalanche effect to fix a voltage at its terminals once the breakdown threshold is reached. When used as voltage clamping device, they are connected as shown in Fig. 2(f), and their electrical characteristics are very similar to those of an MOV. Fig. 9 presents the characteristics of a TVS extracted from datasheet [42] as an example. It is possible to observe a high impedance zone below standoff voltage $V_{\text{STD,OFF}}$ and low impedance zone above breakdown voltage V_{BR}. Some examples of TVS clamps applied to an SSCB are shown in papers [43], [44].

Compared to MOVs, TVSs do not degrade at each surge event (if kept within the datasheet limits). Thus, their lifetime is much longer. Moreover, the transition between the leakage and conduction states of a TVS is much sharper than that of an MOV. Therefore, V_{clamp} changes less with the current level.

One drawback of TVSs, however, is the so-called latch-up effect observed experimentally in [16]. During clamping, some high voltage TVSs exhibit a reduction in V_{clamp} from the initial peak value. If the reduced clamping voltage happens to fall below the DC bus voltage, V_{dc}, the device enters a latch-up state and the current cannot be turned off, leading to the thermal runaway of the components. Therefore, during the selection of TVS snubbers, a sufficient margin from V_{dc} should be accounted for to completely avoid the latch-up. This in turns means that a TVS with a higher voltage rating than strictly required has to be selected, and thus a higher clamping voltage should also be expected. Moreover, being based purely on silicon and controlled doping processes, high power TVSs are very expensive and therefore not as widespread as MOVs.

D. ACTIVE CLAMP

An interesting clamping technique that is found in the literature is the so-called *"active clamp"* (Fig. 10). Papers [45], [46], and [47] analyze this solution in detail. This kind of clamp requires a "voltage sensing component" such as an MOV or a TVS to be connected between the drain/collector of the power electronic device and the gate.

This MOV or TVS provides feedback to the gate voltage, which prevents the SSCB MOSFETs or insulated-gate bipolar transistors (IGBTs) from being turned off completely and drives them into the active region for a given amount of time. In this clamp, the voltage between the collector/drain and emitter/source is fixed by the MOV or TVS clamping voltage plus the gate voltage. The line energy is then dissipated through the heatsink of the power electronic devices. This technique is sometimes also referred to as *"snubberless"* because no additional snubber circuit is used to absorb/dissipate the inductive energy. It must be noted that this is the most compact type of clamping technique and requires a smaller number of components rated for low energy compared to other passive snubbers. However, as proven in [47], the amount of energy that can be dissipated inside the power electronics during turn off is limited by the thermal impedance of the semiconductor. Thus, the maximum amounts of load/line inductance and resistance must be carefully considered to avoid the thermal destruction of the SSCB. Nonetheless, this solution could yield interesting results when combined with any other snubber presented up to now. In particular, the fast and direct action on the gates of the power electronic switches makes it possible to mitigate the first voltage overshoot above V_{clamp}, which always occurs as a result of the parasitic inductance present in the commutation path between the snubber and SSCB.

E. GAS DISCHARGE TUBE AND DISSIPATIVE ELEMENT

This section presents a solution that uses a gas discharge tube (GDT) or spark gap, plus a dissipative element such as an MOV, as reported in Fig. 11.

The idea behind this solution was inspired by the spark gap plus varistor arrester used for lightning surge protection in transmission lines. This solution tries to address the problem of MOV leakage current at the DC bus voltage by connecting a spark gap, which sustains most of the DC voltage, in series with the MOV. The working principles of the GDT +

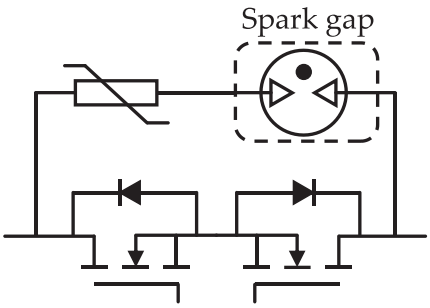

FIGURE 11. Example of GDT+MOV snubber scheme.

TABLE 2. System Parameters Used for Simulations

Parameter	Value	Description
V_{dc}	500 V	Nominal bus voltage
V_{dss}	1200 V	Semiconductor breakdown voltage
L_{fault}	50 µH	Fault inductance
I_n	50 A	Nominal SSCB current
I_{trip}	350 A	SSCB trip threshold

MOV are as follows. When the SSCB needs to be opened, the voltage across the spark gap increases as a result of the line inductance until the striking voltage of the gap is reached. At that point, the voltage on the gap drops significantly as a conductive channel in an ionized gas is created. Thus, the MOV is connected to the SSCB and starts conducting a current, clamping the voltage to the desired level. When the current is reduced to zero, the ionized gas recovers its dielectric properties, and the spark gap starts blocking its share of the DC bus voltage again. However, some drawbacks are the low durability of the GDT after several turn-off events during its lifetime, and the difficulty of accurately representing the complex phenomena describing the GDT behavior during ignition. On the latter matter, in [48], Zola proposed a simplified model using SPICE electronic components.

It should be noted that the GDT cannot work alone as a voltage snubber for an SSCB because after the arc strike, the voltage drops to a low value. Thus, it cannot turn off the current and isolate the fault in a reasonable amount of time.

In [49], Liu et al. proposed a *"gapped MOV"*. The peculiarity of the gapped MOV is that it employs some spark gaps carved directly into the MOV material. The results reported in [49] showed an increase in the voltage utilization of the switch from 44% with a simple MOV to 72% with a gapped MOV. The paper also provides insight on the dynamic behavior of the voltage clamp, as well as the modeling of the spark gap. However, the lifetime problem still remains because of the open-air nature of the device.

F. FREEWHEELING CLAMP

The last snubber analyzed in the basic snubber category is the so-called *freewheeling snubber*. This kind of snubber uses a shunt element across the line poles (or line to ground) to redirect a fault current and help the SSCB switch off and isolate the source from the fault. This clamping technique is simple to implement, and the working principle is the same as that of the freewheeling diode typically applied on inductive loads. One drawback of this solution is that it requires more components to be bidirectional (i.e., to be effective for both load side and source side faults) and, depending on the components used, it may not accept reverse voltage polarity.

Papers [50] and [51] proposed and analyzed different variations of this kind of voltage clamping method. In [50], several examples of this kind of clamp were considered and compared with the typical snubbers used for SSCBs such as MOVs and RCD snubbers. The simplest form of freewheeling snubber consists of a diode shunt connected to the line on the load side with appropriate polarity. In this way the SSCB switch is only subjected to the overvoltage caused by the source-side inductance, which can be minimized by placing the SSCB very close to the supply or adopting a source bypass capacitor to divert the source inductance current away from the SSCB. The diode can be replaced with a shunt MOV or a combination of both to reduce the fault current quicker. Indeed, a simple freewheeling diode would not be suitable for an SSCB snubber because the fault inductance energy is not efficiently dissipated and too much time would be required to clear the fault. In the latter cases, however, the SSCB is subjected to a voltage equal to $V_{dc} + V_{clamp}$. Fig. 12 shows the mentioned topologies.

In [52], the effect of a source-side inductance was analyzed, and it was found that an RCD snubber was required to avoid overvoltages in the case of a source-side fault. In this case, a resistor was placed in series with the freewheeling diode, instead of an MOV, to dissipate the inductive energy. Its value had to be sized to limit the voltage drop at the maximum fault current below the breakdown of the SSCB components. Another example of a freewheeling snubber used in combination with an RC snubber is shown in Fig. 13 [53]. In this solution, a diode with a resistor is connected between the poles of the line and the ground after the SSCB. The fault current on the line can recirculate in the diode path, and the inductive energy is dissipated by the resistor. In this way, the current in the RC snubber is lower, and thus its design is efficient.

IV. INTERRUPTION CHARACTERISTICS AND COMPARISON OF BASIC SNUBBER CONCEPTS

We next discuss the interruption waveforms for the basic snubber concepts. These graphs are qualitative and serve to represent how the different snubbers behave relative to each other for a given interruption condition.

Figs. 14 and 16 show the clamping voltage waveforms at turn off, while Figs. 15 and 17 show the line current waveforms in the same time window.

The system parameters used for the simulations are reported in Table 2, while the most relevant snubber parameters

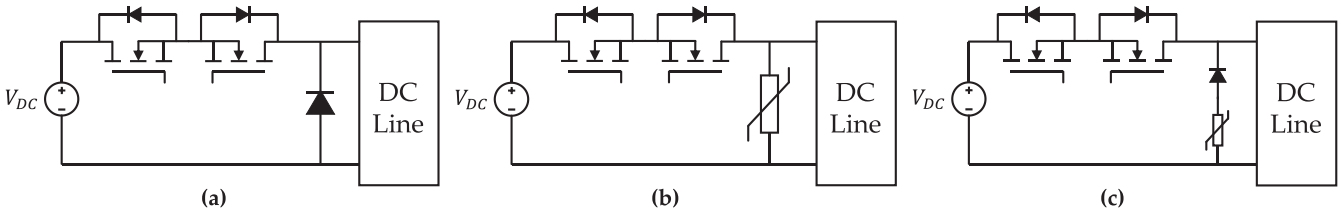

FIGURE 12. Example of freewheeling snubbers: (a) freewheeling diode, (b) freewheeling MOV, and (c) freewheeling MOV + diode. [50].

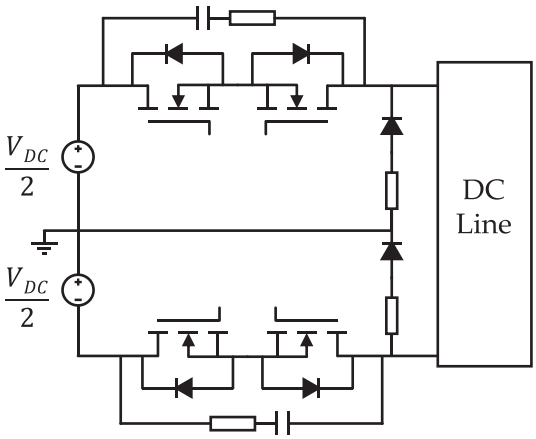

FIGURE 13. Example of freewheeling snubber + RC from [53].

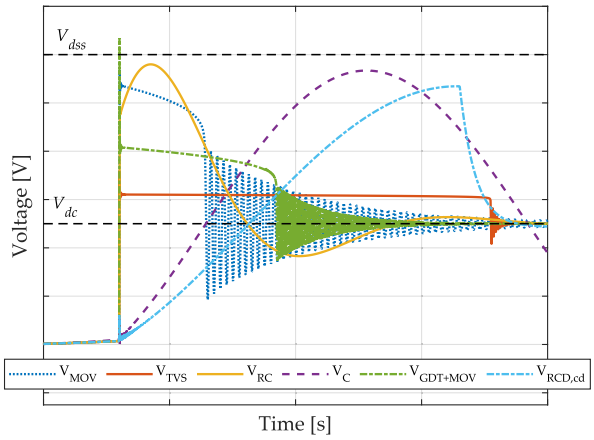

FIGURE 14. Basic snubbers clamping voltage waveforms: MOV, TVS, RC, C, GDT+MOV, and RCD charge-discharge type (RCD,cd).

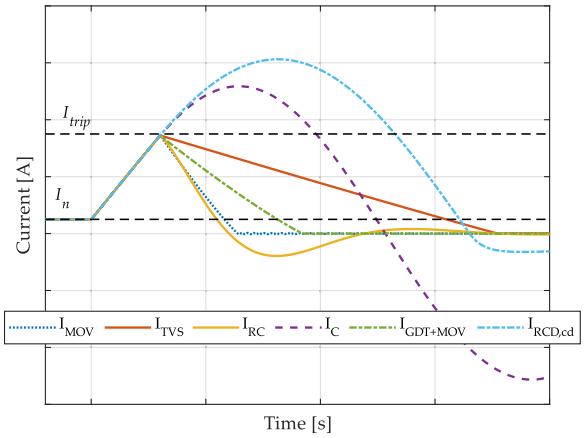

FIGURE 15. Basic snubber line current waveforms: MOV, TVS, RC, C, GDT+MOV, and RCD charge discharge type (RCD, cd).

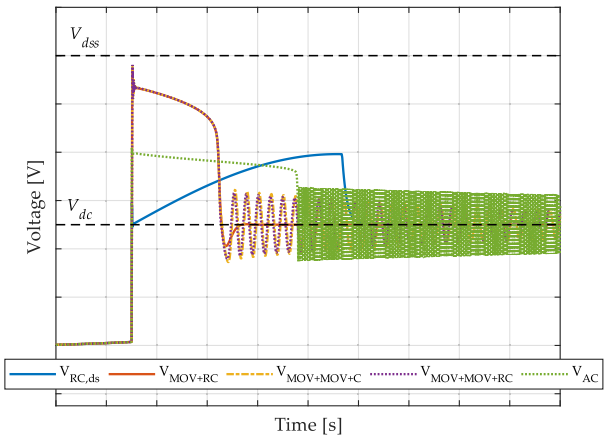

FIGURE 16. Basic snubber clamping voltage waveforms: RCD discharge suppress type I (RCD,ds), MOV+RC, MOV+MOV+C, MOV+MOV+RC, and active clamp (AC).

for each presented architecture are reported in Table 3. Table 4 summarizes some remarks that can be drawn from the graphical comparison presented in Figs. 14 to 17.

In general, as expected, a higher clamping voltage leads to a shorter time required to clear the fault. Moreover, it is possible to see that snubbers that make use of a capacitor that charges during the turn-off process (C snubber and RCD *charge–discharge* type) have a line current that keeps flowing beyond the tripping threshold (purple dashed and light blue dash-dotted lines in Figs. 14 and 15, respectively). This is because the current cannot stop increasing until the voltage across the SSCB has reached at least V_{dc}.

Indeed, the impact of this issue is clearly visible when considering the RCD discharge suppressing-type snubber (blue solid line in Figs. 16 and 17), where the capacitor is kept charged, and thus the current stops increasing as soon as the SSCB is turned off. This issue, which is not present in the other snubbers, means that at turn off, the C and RCD *charge-discharge* type snubbers have to be designed to dissipate an energy greater than the value strictly required at turn off. In addition, the C snubbers present undamped oscillations after the SSCB has turned off, which implies that quite some time must pass before the fault current is effectively cleared. Thus,

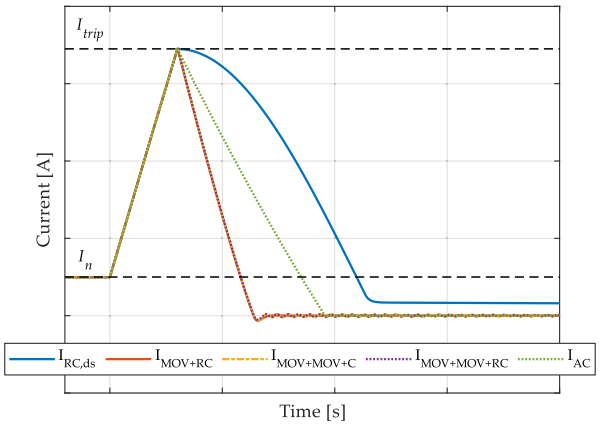

FIGURE 17. Basic snubbers line current waveforms: RCD discharge suppress type I (RCD,ds), MOV+RC, MOV+MOV+C, MOV+MOV+RC, and active clamp (AC).

TABLE 3. Snubber Parameters Used for Simulations

Clamp Type	Parameters
MOV	V_{dc} = 585 V, V_{clamp} = 1200 V
TVS	V_{dc} = 550 V, V_{clamp} = 663 V
RC	R = 2.7 Ω, C = 5.6 µF
C	C = 33 µF
GDT+MOV	$V_{dc,GDT}$ = 250V, $V_{dc,MOV}$ = 369 V, $V_{clamp,MOV}$ = 690 V
RCD charge discharge	R = 8.2 Ω, C = 56 µF
RCD discharge suppress type I	R = 27 Ω, C = 56 µF
MOV+RC	$V_{dc,MOV}$ = 585 V, $V_{clamp,MOV}$ = 1200 V R = 47 Ω, C = 56 nF
MOV+MOV+C	$V_{dc,MOV1}$ = 585 V, $V_{clamp,MOV1}$ = 1200 V C = 56 nF V_{dcMOV2} = 175 V, $V_{clamp,MOV2}$ = 345 V
MOV+MOV+RC	$V_{dc,MOV1}$ = 585 V, $V_{clamp,MOV1}$ = 1200 V R = 10 kΩ, C = 56 nF V_{dcMOV2} = 175 V, $V_{clamp,MOV2}$ = 345 V
Active clamp	V_{clamp} = 660 V

the performances of the whole system are negatively impacted as the DC link capacitors keeps on discharging and the load cannot be reconnected for a long time. This problem is resolved in the RCD snubber, both in the *charge-discharge* and *discharge-suppressing* types, because the diode prevents the current from oscillating back and forth. Nonetheless, the design of C and RCD snubbers is mainly driven by the capacitor sizing. Capacitors are available with several current and voltage ratings. However, when considering the amount of energy to be stored, the volume becomes impractical for many applications. In conclusion, the C snubber is never used because its non-dissipative nature makes it unsuitable for SSCB applications. Even if the volume was acceptable and long-lasting oscillations were not an issue, a C snubber causes a huge current spike at SSCB turn on, which can cause false trips of the breaker. Both of the RCD snubber types mitigate this issue with the inclusion of a resistor in the capacitor path. Regarding the clamping performances, the *discharge-suppressing* type is preferred over the *charge-discharge* type because it is capable of stopping the current increase as soon as possible. Thus, less energy is stored in the system inductance, which in turn helps with the capacitor design. The only drawback of the *discharge-suppressing* RCD snubber, as already mentioned, is the direct connection of the DC line poles through the snubber components, which may increase the risks of discharge. One further remark about RCD snubbers is that the resistor plays a role in the resetting time required to restore the initial conditions, i.e., charging the capacitor to V_{dc} in the RCD *charge-discharge* type and discharging the capacitor to V_{dc} in the RCD *discharge-suppressing* type. This also impacts the time that must pass in order to be able to reconnect the systems to the supply.

The behavior of an RC snubber (yellow solid line in Figs. 14 and 15) is different from that of C and RCD clamps. The current cuts off immediately after turn off, and the voltage has lower oscillations. However, the resistor is connected in series to the commutation path. Thus, an ohmic voltage drop is added to the clamping voltage. This aspect significantly limits the turn-off capability of the SSCB. Indeed, depending on the desired tripping threshold, there is a maximum allowed resistance value that can be used. Moreover, this can be especially problematic when considering a high slope fault current, where the actual peak turn-off current may exceed the tripping threshold by several factors because of the delay between detection and tripping. This requirement also conflicts with the necessity of decreasing the turn-on current spike from the capacitor. Therefore, the RC snubber is rarely used.

Regarding the other snubber types that use an MOV as a dissipating element, their behaviors are similar in relation to the clamping voltage, with the differences basically related to the amount of ringing at turn off and the peak clamping voltage value. Snubbers of types MOV + RC (orange solid line in Figs. 16 and 17), MOV + MOV + C (yellow dash-dotted line in Figs. 16 and 17), and MOV + MOV + RC (purple dotted line in Figs. 16 and 17) all exhibit more damping in the oscillations than a simple MOV (blue dotted line in Figs. 14 and 15). However, the actual impact depends on the values chosen for the different elements. The GDT + MOV type (green dash-dotted line in Figs. 14 and 15) can use a lower rated MOV, but the spark trigger dynamic introduces a very high initial voltage spike above V_{dss}, even if just for a few tens of nanoseconds. This spike, depending on the semiconductor

TABLE 4. Basic Snubber Remarks

Snubber Type	Time Duration of Oscillations	Switch Voltage Utilization Ratio	Notes
C	Extremely long	Very high	–
RC	Short	Very high	Ohmic voltage drop
MOV	Medium	High	–
TVS	Short	Lowest	Possible foldback of clamping voltage
GDT+MOV	Medium	Highest	Voltage spike above V_{dss}
RCD charge discharge type	No oscillations	Medium	–
RCD discharge suppressing type	No oscillations	Low	–
MOV+RC	Very short	High	–
MOV+MOV+C	Medium	High	–
MOV+MOV+RC	Medium	High	–
Active clamp	Very long	Low	Dissipate all the energy in the semicondutor

technology used, can be detrimental to the overall reliability as the dies termination region gets stressed beyond the design specifications. To mitigate this, either another snubber is used in parallel, such as an RC cell or active clamp, or the SSCB has to be slowed down during turn off. The inclusion of a GDT improves the switch voltage utilization ratio with respect to the simple MOV snubber. However, the degradation of the spark gap, which is typically rated for 10 operations at full current, is the limiting factor.

Finally, we analyze the TVS (orange solid line in Figs. 14 and 15) and active clamp (green dotted line in Figs. 16 and 17), which showed similar behaviors in relation to the clamping voltage and managed to reach a lower switch voltage utilization ratio in this simulation. However, the active clamp has the big drawback of dissipating all the inductive energy inside the semiconductor. Depending on the line/fault inductance, this may not be viable at all and would require another dissipation device with a higher rating in parallel, which would defeat its purpose as a single compact solution. Therefore, the active clamp is recommended for use in coordination with another snubber to avoid excessive thermal stress on the power electronics. The behavior of the TVS clamp is similar to that of an MOV, with a flatter clamping voltage; the only issue with this technology is the lower energy rating of the component compared to an MOV. Moreover, the foldback effect is not modeled in practice. Thus, the switch voltage utilization ratio may end up being higher than expected. Nonetheless TVSs are good alternatives when the clamping voltage of an MOV cannot be less than V_{dss} while keeping its nominal voltage above the system voltage, V_{dc}.

V. ADVANCED CONCEPTS FOR VOLTAGE CLAMPING

This section outlines some solutions that require a modification of the typical SSCB topology. In addition, some advanced architectures that use controlled components are presented. These snubbers have particularly been studied for SSCBs in order to address some of the criticalities of previous solutions.

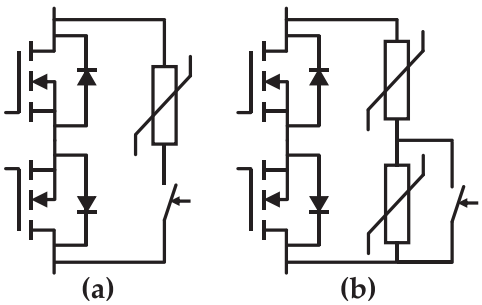

FIGURE 18. Snubber topologies applied to a MOSFET bidirectional SSCB: (a) MOV+Switch, and (b) MOVs+Switch alternative [54].

A. ACTIVELY CONTROLLED SNUBBERS

The category of actively controlled snubbers includes devices that use some controlled switches to connect or disconnect the energy dissipation element at will.

Patent [54] shows some examples of actively controlled snubbers (Fig. 18(a) and (b)). The idea is to make use of a controlled switch (typically another power electronic device) to reduce the leakage of the MOV during the OFF state of the SSCB. The working principle of both is to turn on the controlled switch together with the SSCB and turn it off with a controlled delay with respect to the main SSCB turn off after the fault energy has been dissipated. In this way, the MOV can be properly connected in parallel to the SSCB to control the voltage across it and dissipate the fault energy. Moreover, it is also possible to lower the MOV voltage rating because the DC bus voltage is shared with the switch. It is clear that having a controlled switch inside the voltage clamp

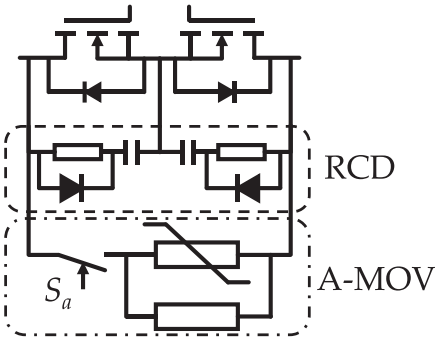

FIGURE 19. Actively controlled snubbers presented in [55]: AMOV-RCD.

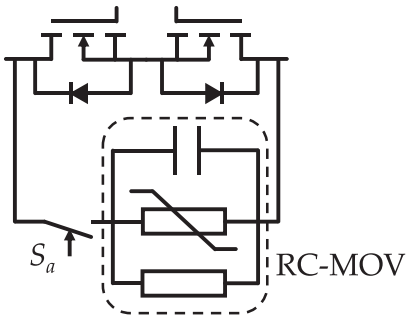

FIGURE 20. Actively controlled snubbers presented in [55]: RCS-MOV.

and the need to synchronize the commutation with the SSCB greatly increases the complexity of the solution and adds a safety hazard should the snubber switch fail for some reason. In that case, the inductive energy would not find the intended dissipation path and some damage could occur. For this reason, a suitable fail-safe mechanism should be used so that without any control action, the snubber is in a condition that does not present any risk of damaging the SSCB and nearby equipment.

Two novel actively controlled snubbers were proposed in [55] by Kheirollahi et al. as follows:

- RCD + Active MOV (AMOV-RCD),
- RC + switch +MOV (RCS-MOV).

These topologies, which are represented in Figs. 19 and 20, respectively, combine a passive snubber (i.e., MOV+RC) and controlled switch. The switch is used, again, to disconnect the clamping circuit from the DC bus in order to preserve the energy dissipating element, which in both cases is an MOV. Auxiliary switch S_a can be either a fully controlled (i.e., a MOSFET) or half-controlled switch (i.e., a thyristor). With a fully controlled switch, S_a is turned on together with the SSCB and turned off after the inductive energy has been dissipated. In contrast, with a half-controlled switch, the turn on has to be triggered at the SSCB turn off, and the turn off will occur naturally after the line current is driven to zero.

In addition, in these two cases, the need for additional gate driving components and the need to synchronize the commutation of the S_a increase the complexity of the solutions.

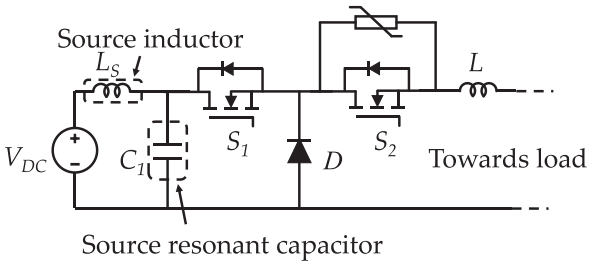

FIGURE 21. Example of surgeless clamp proposed in [56].

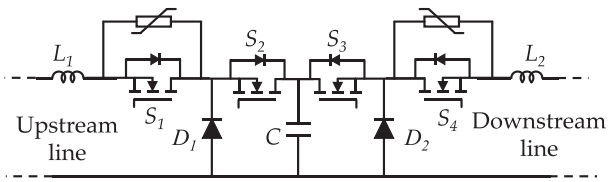

FIGURE 22. Example of bidirectional surgeless snubber proposed in [56].

B. SURGELESS VOLTAGE CLAMPS

We next present a particular type of voltage clamping that is very similar to the freewheeling snubber. It is called a *"Surgeless voltage clamp"* which is a term that was initially introduced in [22] by Sano et al. to define any topology that allows the main SSCB switches to commutate without an overvoltage or with a voltage fixed to a level that is predetermined by the designer.

In [56], Pang et al. proposed the surgeless snubber reported in Fig. 21. The resemblance to the freewheeling snubber is clear, and the working principle is the same: divert the current away from the commutating branch. This time, however, the diode has a slightly different placement with respect to the freewheeling cases. Moreover, the whole SSCB undergoes substantial changes with respect to the typical topology. Thus, this snubber architecture is worth further discussion. In particular, in this solution, the SSCB switch is split into two, with the diode placed between them. In this way, the source is bypassed by the diode, and S_1 can turn off without any overvoltage, while the varistor in parallel to S_2 absorbs all the inductance energy when it is turned off. It must be noted that to avoid overvoltages on S_1 at turn off, a shunt capacitor connected before the switch is required to recirculate the source inductance current. A bidirectional solution was also presented with the same concept and is shown in Fig. 22. This technique makes it possible to choose a voltage class for the main SSCB components that is as close as possible to the DC bus voltage because the fault inductor voltage will not be added to the supply voltage to create a high overshoot on power electronic switches. In contrast, the size of S_2 is only based on the selected clamping voltage value. The topology presented by Pang et al. has only been tested in a lab and should be investigated further in field applications where system parameters may be not fully known in order to determine the real performances. The main critical point involves the source resonant capacitor, which, as with the C and RCD

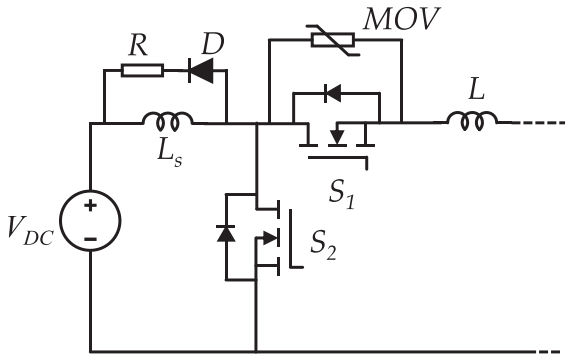

FIGURE 23. Example of modified surgeless clamp proposed in [57].

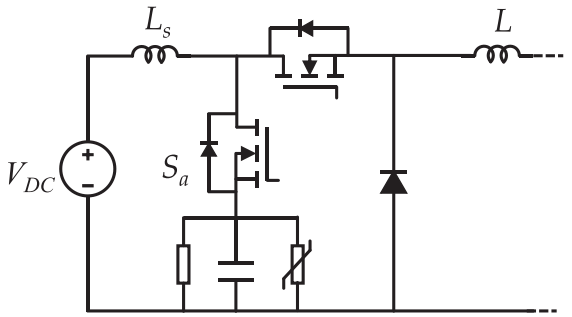

FIGURE 24. Actively controlled surgeless snubber + freewheeling snubber presented in [58].

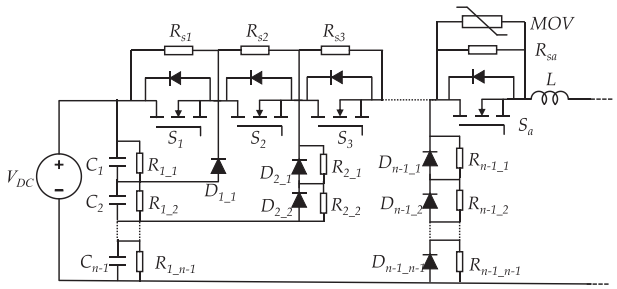

FIGURE 25. General structure of multilevel surgeless clamp proposed in [59].

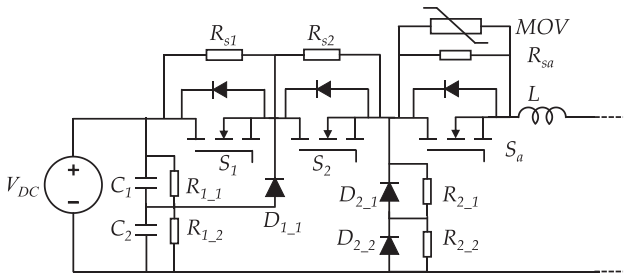

FIGURE 26. Surgeless clamp proposed in [59] with n = 3.

charge-discharge-type snubbers, has to be designed to contain the voltage increase according to the energy stored in the source inductance. Unless the source inductance value can be controlled, the value of this capacitor would be impractically large in many applications.

In [57], a similar concept was presented that made use of a current limiting circuit and an additional semiconductor switch (called a "*Ground clamping switch*") that was triggered after the fault detection to isolate the SSCB from the supply. The schematic is shown in Fig. 23. This solution allows the SSCB to see an overvoltage only as a result of the line inductance, which can be fixed at any desired level by the designer with an MOV or a similar component. It must be noted that to limit the source current flowing into the ground bypass switch, an additional inductor with a freewheeling diode must be used. This solution is not bidirectional. Another similar design was also proposed in [58] to address the source inductance energy. This solution includes a source bypass circuit consisting of an RC cell, a varistor, and an active switch, as represented in Fig. 24. The idea here is to close switch S_a and open the main SSCB pole in order to divert the source inductance current into the RC+MOV cell. In addition, the solution has a freewheeling diode to cope with the line fault current.

As a further evolution of the concept presented in [56], Pang et al. proposed a new topology for a surgeless SSCB in [59]. This time, the study focused on a medium-voltage SSCB where, typically, several switches in series are needed to block the DC bus voltage, and the problem of dynamic voltage sharing among components during turn off is quite critical. In this solution, the surgeless effect was achieved thanks to a network of capacitors and diodes. The general topology composed of n cells is reported in Fig. 25. The structure is composed of *n-1* auxiliary switches in series (S_1 … S_{n-1}), plus one main switch, S_a, that has an MOV in parallel. Then, n capacitors are connected in parallel with the DC supply, which will charge up to $V_{dc}/(n-1)$. The n^{th}-*1* capacitor is then connected across the n^{th}-*1* switch through *n-1* diodes. The last diode chain will connect the positive pole to the negative pole, creating a freewheeling path right before switch S_a.

The working principle can be understood more easily with reference to Fig. 26, where $n = 3$. When the SSCB needs to be tripped, the switches are turned off sequentially, with S_1 opened first. In that case, the fault current commutates through capacitor C_1 and, thanks to diode D_{1_1}, keeps flowing through S_2. Because C_1 is charged at $V_{dc}/2$, no overvoltage is seen by S_1. The same occurs when opening S_2. At this point, a freewheeling action occurs thanks to D_{2_1} and D_{2_2}, and lastly the fault current can be dissipated inside the MOV after opening S_a. This solution has been proven to be scalable to a very high value of n and to have a faster isolation speed compared to the more basic series connection of switches, with each one clamped with a varistor. A bidirectional solution was also presented in the same paper, mirroring the structure with respect to the capacitors.

C. "ELECTRONIC" MOV

The solution presented in [60] by Lakshmi et al. tries to address several problems that arise when using an MOV

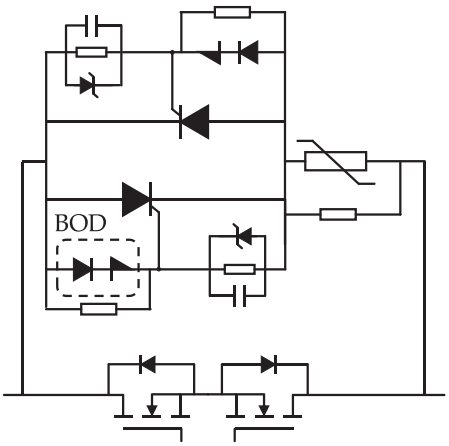

FIGURE 27. Example of electronic MOV proposed in [60].

for clamping an SSCB. It is well known that MOVs are exceptional at absorbing high amounts of energy. However, their continuous rated power is very low (on the order of a few watts). Therefore, care must be taken when selecting the component so that DC bus voltage V_{dc} falls far below MOV nominal voltage V_v (i.e., MOV voltage at 1 mA) to limit the leakage current and thus the continuous dissipated power. At the same time, as previously said, maximum clamping voltage V_{clamp} must not exceed the breakdown voltage of the power semiconductor used. Typical values from manufacturer datasheets show that the maximum V_{clamp} value is approximately 2–3 times the maximum rated DC voltage of the MOV. However, this value depends strongly on the current that is expected to flow. Often, it is not possible to find a component that satisfies both constraints; therefore, the only solution is to reduce the DC bus voltage and/or increase the voltage class of the components. Putting more MOVs in series/parallel could be a solution to shape the *V–I* curve as desired, even though it has been shown to yield unsatisfactory results. Indeed, as the number of MOVs in series/parallel increases, there is a higher risk of unbalanced voltage/current sharing, leading to the early failure of the whole snubber.

Lakshmi et al. proposed a solution that continues to use an MOV as the main absorbing element to dissipate the inductive energy. However, it is now combined with a "triggering" cell in series. This cell consists of a thyristor and an avalanche breakover diode (BOD), plus some passive components to protect the thyristor gate. Moreover, some resistors are used to address the steady state voltage sharing. The scheme of this device is represented in Fig. 27.

The architecture is an evolution of the active MOV concept presented in [55]. Here, the main novelty is the self-triggering mechanism of the series switch, which removes the need for a separate gate driver and reduces the overall complexity of the solution, while increasing the reliability.

The working principle of this electronic MOV (*eMOV*) can be expressed as follows:

- at a steady state with the SSCB open, the voltage is shared by the MOV and BOD, thus reducing the leakage current of the MOV;
- when the SSCB is conducting and receives a trip command, part of the current commutates through the BOD and the auxiliary thyristor gate components (resistor, capacitor, and Zener diode), while part of the current keeps flowing through the IGBT/MOSFET parasitic capacitance; when a sufficient thyristor gate voltage is reached, the component is fired and directly connects the MOV in parallel to the SSCB;
- at this moment, the current starts decreasing and inductive energy is dissipated inside the MOV;
- when the current decreases to less than the holding current of the thyristor, the snubber switches off and static voltage sharing is established thanks to some balancing resistors.

This solution can effectively help relieve some of the constraints when designing a snubber for an SSCB, allowing a great degree of flexibility when decoupling the off (leakage) performances from the on (clamping) performances. Moreover, the added components do not require controlled triggering circuitry because the firing of the thyristor is managed by the BOD itself, which greatly simplifies the design. One disadvantage of this contraption is the relatively long time typically required for the thyristor to turn completely on. This delay in the insertion of the MOV may lead to a higher peak current at turn off when a short circuit is detected. The solution proposed in [60] is also bidirectional thanks to the antiparallel thyristor and triggering cell.

VI. FINAL COMPARISON AND GUIDELINES

After presenting the advanced concepts for SSCB voltage clamping architectures, it is now possible to proceed with an overall comparison.

As already mentioned, all of the advanced concepts aim to improve on the shortcoming of the basic snubber concepts. In particular, the target is to achieve the lowest switch voltage utilization ratio possible in order to reduce SSCB overdesign in term of the breakdown voltage. In Table 5, a final summary is provided. This table collects and compares briefly all the snubber concepts that have been discussed in this paper.

All the solutions belonging to the "*advanced concepts*" category presented in this article use an MOV as the main dissipation element and work around that to achieve an improved behavior in terms of the voltage switch utilization ratio and ringing at turn off. It is therefore natural to compare the novel architectures against the MOV snubber, which is taken as the benchmark device.

There are two main lines of thought among the different approaches presented for the "*advanced concepts*" both of which try to extend the operating region of the MOV:

- using an element in series with the MOV to share the DC blocking voltage and reduce the leakage current and power dissipated at idle in the MOV (Figs. 18–20 and 27);

TABLE 5. Comparison Summary of all Snubber Concepts

Snubber Type	Minimum No. of Components (for bidirectional snubber)	Energy Handling Capability	Current Handling Capability	Passive	Switch Voltage Utilization Ratio	Oscillations Damping After Turn Off	References
C	1	2	2	YES	1	1	[16]
RC	2	3	2	YES	2	3	[16]
RCD *charge discharge* type	6	3	4	YES	2	5	[16], [17], [25], [26]
RCD *discharge suppressing* type	6	4	3	YES	3	5	[16], [25]-[27], [40]
MOV	1	4	4	YES	3	3	[16]-[19], [36]-[41][40]
MOV+RC	3	4	4	YES	3	5	[16]-[19]
MOV+MOV+RC	4	5	5	YES	3	5	[24]
MOV+MOV+C	3	5	5	YES	3	4	[16], [23]
TVS	1	3	5	YES	5	4	[16], [43], [44]
Active clamp	2	1	3	YES	5	2	[45]-[47]
GDT+MOV	2	5	5	YES	4	3	[49]
Freewheeling	2	2	3	YES	5	5	[16], [50]-[53]
AMOV+RCD	5	5	5	NO	4	3	[55]
RCS+MOV	4	5	5	NO	4	3	[55]
Surgeless	5	3	4	NO	5	5	[56]-[59]
eMOV	14	5	5	YES	4	5	[60]

- creating a secondary path to divert the fault current and enable the downsizing of the MOV (Figs. 23–26).

The first group of architectures has the advantage of being a natural evolution of an MOV snubber, but the implementations are not trivial. Moreover, in the case of a malfunction, the clamping action is not guaranteed unless a topology such as that in Figs. 18(b) or 19 is used, where a "conventional" snubber is still present. Still, the desired clamping performances may not be achieved and some damage could occur to the SSCB. Nonetheless, these solutions allow a low switch voltage utilization ratio of 1.4–1.6.

The second group of architectures is closer to the freewheeling snubber. Indeed, there is still a path to recirculate the fault/line current, either through a diode or controlled switch. Again in this case, the need for additional gate driving increases the complexity and reduces the reliability of the SSCB. However, one advantage that is gained by isolating the DC supply from the load through the controlled switch or diode is that the energy requirement for the dissipation devices decreases from (1) to just the energy stored inside the fault/line inductance. This can be clearly seen if V_{dc} is replaced by zero in the equation.

Regarding the oscillation at turn off, the behavior is identical to the MOV or MOV + RC. Therefore, no further comments will be made.

Based on the previous discussion, it is now possible to define some guidelines for selecting voltage clamping devices.

The design should start by determining the following values:

- trip current;
- expected maximum and minimum *di/dt*;
- maximum expected time delay t_d between sensing and tripping;
- SSCB breakdown voltage;
- DC line voltage.

Knowing the expected maximum and minimum *di/dt* values, together with the DC line voltage, make it possible to define the maximum and minimum expected fault and line inductance values as follows:

$$L_{\min/\max} = \frac{V_{dc}}{di/dt\Big|_{\max/\min}}. \tag{3}$$

Then, the peak trip current can be computed as with the time delay and maximum current slope:

$$I_{peak} = t_d \left.\frac{di}{dt}\right|_{\max}. \tag{4}$$

It is now possible to obtain a rough estimation of the required energy to be dissipated inside the clamping system

using (1), considering the semiconductor breakdown voltage as the clamping voltage.

Generally speaking, if the resulting energy is on the order of kilojoules and the peak current is on the order of a few kiloamps, the snubber will definitely need an MOV as a dissipating element. Whether a simple MOV or a more advanced concept is necessary will depend on the voltage switch utilization ratio available (V_{clamp} over V_{dc}). For values above 2, a simple MOV solution is enough, while for values below 2 but above 1.4, a more advanced architecture must be used. For example, for a GDT + MOV (with means to control the initial spark triggering overvoltage), an *eMOV* or an actively controlled snubber may suit the application. Moreover, it is possible to reduce the energy requirements for the dissipating element by using a topology that separates the supply from the fault/load, i.e., a *surgeless* topology or an actively controlled snubber with a ground clamping switch.

Then, in a case where the energy requirement is on the order of hundreds of joules and the peak current is on the order of a few kiloamps, the best choice could be the TVS or RCD *discharge-suppressing* type, with the TVS being the best in a case where the lowest voltage switch utilization ratio is needed.

Finally, for systems where the energy to be dissipated is less than a few hundred joules and the peak current is on the order of hundreds of amps, the optimal choice would be a simple RC snubber or an active clamp, where the active clamp achieves the lowest voltage switch utilization ratio between the two solutions.

It must be noted that being largely diffused, available in several ratings and cheap, the MOV can be adopted for almost any application provided that the voltage switch utilization ratio is high enough.

VII. CONCLUSION

In this paper, several voltage clamping techniques have been analyzed and their advantages and disadvantages have been summarized and compared. We started with the most classic solutions such as C, MOV, TVS, and RCD snubbers and then discussed more advanced concepts such as actively controlled snubbers and the *eMOV* concept. The work presented in this paper highlighted that an effort is being made by the scientific community to achieve a small voltage utilization ratio in order to reduce the overdesign of the semiconductor switches inside SSCBs. MOVs are still a very popular solution thanks to their availability, design simplicity, and energy absorption capability. However, most of the time, a simple MOV is not able to limit the overvoltages below the breakdown of the SSCB and still have a low leakage current when the full DC bus voltage is applied. In this regard, some solutions presented in the literature try to disconnect the MOV from the line to reduce the leakage current and then connect it to the SCCB only when needed, such as when using the GDT + MOV combination. This concept is also the focus of solutions such as the "*eMOV*" [60] and "*gapped MOV*" [49], where the authors used this idea in an innovative way. The use of auxiliary power electronic components or spark gaps to disconnect the MOV from the SSCB is a promising solution to achieve the overall desired performances. Nonetheless, improvements in passive solutions such as the RCD *discharge-suppressing* type, and all the architectures that include a main MOV for dissipating the energy and auxiliary components to control the oscillations at turn off, may still be good candidates for applications where the requirements are not too stringent. Finally, transient voltage suppression diode-based snubbers provide good electrical performances in terms of the clamping voltage but sacrifice the energy dissipation capability. TVSs shine in applications where the lowest switch voltage utilization ratio has to be achieved and the fault/line inductance is not very high.

REFERENCES

[1] K. Shimomachi, R. Hara, and H. Kita, "Comparison between DC and AC microgrid systems considering ratio of DC load," in *Proc. IEEE PES Asia-Pacific Power Energy Eng. Conf.*, 2015, pp. 1–4, doi: 10.1109/APPEEC.2015.7380918.

[2] T. Kuhlmann, I. Bianchini, and A. Sauer, "Resource and energy efficiency assessment of an industrial DC Smart Grid," *Procedia CIRP*, vol. 90, pp. 672–676, 2020, doi: 10.1016/j.procir.2020.01.074.

[3] L. Xu et al., "A review of DC shipboard microgrids—Part I: Power architectures, energy storage, and power converters," *IEEE Trans. Power Electron.*, vol. 37, no. 5, pp. 5155–5172, May 2022, doi: 10.1109/TPEL.2021.3128417.

[4] L. Xu et al., "A review of DC shipboard microgrids—Part II: Control architectures, stability analysis, and protection schemes," *IEEE Trans. Power Electron.*, vol. 37, no. 4, pp. 4105–4120, Apr. 2022, doi: 10.1109/TPEL.2021.3128409.

[5] S. Kim, S.-N. Kim, and D. Dujic, "Extending protection selectivity in DC shipboard power systems by means of additional bus capacitance," *IEEE Trans. Ind. Electron.*, vol. 67, no. 5, pp. 3673–3683, May 2020, doi: 10.1109/TIE.2019.2916371.

[6] M. Mosayebi and M. H. Khooban, "A robust shipboard DC-DC power converter control: Concept analysis and experimental results," *IEEE Trans. Circuits Syst. II: Exp. Briefs*, vol. 67, no. 11, pp. 2612–2616, Nov. 2020, doi: 10.1109/TCSII.2019.2963648.

[7] D. Talapko, "Telecom datacenter power infrastructure availability comparison of DC and AC UPS," in *Proc. Intelec*, 2012, pp. 1–5, doi: 10.1109/INTLEC.2012.6374509.

[8] M. Salato, A. Zolj, D. J. Becker, and B. J. Sonnenberg, "Power system architectures for 380V DC distribution in telecom datacenters," in *Proc. Intelec*, 2012, pp. 1–7, doi: 10.1109/INTLEC.2012.6374469.

[9] M. Tariq, A. I. Maswood, C. J. Gajanayake, and A. K. Gupta, "Modeling and integration of a lithium-ion battery energy storage system with the more electric aircraft 270 V DC power distribution architecture," *IEEE Access*, vol. 6, pp. 41785–41802, 2018, doi: 10.1109/ACCESS.2018.2860679.

[10] N. Swaminathan and Y. Cao, "An overview of high-conversion high-voltage DC–DC converters for electrified aviation power distribution system," *IEEE Trans. Transp. Electrific.*, vol. 6, no. 4, pp. 1740–1754, Dec. 2020, doi: 10.1109/TTE.2020.3009152.

[11] F. S. Al-Ismail, "DC microgrid planning, operation, and control: A comprehensive review," *IEEE Access*, vol. 9, pp. 36154–36172, 2021, doi: 10.1109/ACCESS.2021.3062840.

[12] R. Rodrigues, Y. Du, A. Antoniazzi, and P. Cairoli, "A review of solid-state circuit breakers," *IEEE Trans. Power Electron.*, vol. 36, no. 1, pp. 364–377, Jan. 2021, doi: 10.1109/TPEL.2020.3003358.

[13] "System concept DC-INDUSTRIE2," Accessed: Sep. 04, 2023. [Online]. Available: https://dc-industrie.zvei.org/en/publications/system-concept-for-dc-industrie2

[14] S. Zheng, R. Kheirollahi, J. Pan, L. Xue, J. Wang, and F. Lu, "DC circuit breakers: A technology development status survey," *IEEE Trans. Smart Grid*, vol. 13, no. 5, pp. 3915–3928, Sep. 2022, doi: 10.1109/TSG.2021.3123538.

[15] N. Mohan, T. M. Undeland, and W. P. Robbins, *Power Electronics: Converters, Applications and Design*, 3rd ed. Hoboken, NJ, USA: Wiley, 2003.

[16] X. Song, Y. Du, and P. Cairoli, "Survey and experimental evaluation of voltage clamping components for solid state circuit breakers," in *Proc. IEEE Appl. Power Electron. Conf. Expo.*, 2021, pp. 401–406, doi: 10.1109/APEC42165.2021.9487424.

[17] A. Giannakis and D. Peftitsis, "Performance evaluation and limitations of overvoltage suppression circuits for low- and medium-voltage DC solid-state breakers," *IEEE Open J. Power Electron.*, vol. 2, pp. 277–289, 2021, doi: 10.1109/OJPEL.2021.3068531.

[18] S. Zhao, R. Kheirollahi, Y. Wang, H. Zhang, and F. Lu, "Investigation of limitations in passive voltage clamping-based solid-state DC circuit breakers," *IEEE Open J. Power Electron.*, vol. 3, pp. 209–221, 2022, doi: 10.1109/OJPEL.2022.3163072.

[19] X. Yan et al., "Snubber branch design and development of solid-state DC circuit breaker," *IEEE Trans. Power Electron.*, vol. 38, no. 10, pp. 13042–13051, Oct. 2023, doi: 10.1109/TPEL.2023.3281588.

[20] L. Ravi et al., "Surge current interruption capability of discrete IGBT devices in DC hybrid circuit breakers," *IEEE J. Emerg. Sel. Topics Power Electron.*, vol. 11, no. 3, pp. 3195–3207, Jun. 2023, doi: 10.1109/JESTPE.2023.3264933.

[21] P. C. Todd, "Snubber circuits: Theory, design and application," Unitrode Power Supply Seminar, May 1993, Accessed: Oct. 26, 2023. [Online]. Available: https://www.ti.com/seclit/an/slup100/slup100.pdf

[22] K. Sano and M. Takasaki, "A surgeless solid-state DC circuit breaker for voltage-source-converter-based HVDC systems," *IEEE Trans. Ind. Appl.*, vol. 50, no. 4, pp. 2690–2699, Jul./Aug. 2014, doi: 10.1109/TIA.2013.2293819.

[23] X. Zhang, Z. Yu, Z. Chen, B. Zhao, and R. Zeng, "Optimal design of diode-bridge bidirectional solid-state switch using standard recovery diodes for 500-kV high-voltage DC breaker," *IEEE Trans. Power Electron.*, vol. 35, no. 2, pp. 1165–1170, Feb. 2020, doi: 10.1109/TPEL.2019.2930739.

[24] S. Zhao, R. Kheirollahi, Y. Wang, H. Zhang, and F. Lu, "A diode-free MOV2-RC snubber for solid-state circuit breaker," in *Proc. IEEE Transp. Electrific. Conf. Expo*, 2022, pp. 497–502, doi: 10.1109/ITEC53557.2022.9813936.

[25] D. Shin, S.-K. Sul, J. Sim, and Y.-G. Kim, "Snubber circuit of bidirectional solid state DC circuit breaker based on SiC MOSFET," in *Proc. IEEE Energy Convers. Congr. Expo.*, 2018, pp. 3674–3681, doi: 10.1109/ECCE.2018.8557542.

[26] F. Liu, W. Liu, X. Zha, H. Yang, and K. Feng, "Solid-state circuit breaker snubber design for transient overvoltage suppression at bus fault interruption in low-voltage DC microgrid," *IEEE Trans. Power Electron.*, vol. 32, no. 4, pp. 3007–3021, Apr. 2017, doi: 10.1109/TPEL.2016.2574751.

[27] Z. Wang and E. M. Sankara Narayanan, "Design of a snubber circuit for low voltage DC solid-state circuit breakers," *IET Power Electron*, vol. 14, pp. 1111–1120, 2021, doi: 10.1049/pel2.12092.

[28] "TDK strap varistors model B72240L0751K102 overview," Accessed: Nov. 28, 2023. [Online]. Available: https://product.tdk.com/en/search/protection/voltage/strap-varistor/info?part_no=B72240L0751K102

[29] "TDK strap varistors LS40 series product datasheet," Accessed: Nov. 28, 2023. [Online]. Available: https://product.tdk.com/system/files/dam/doc/product/protection/voltage/strap-varistor/data_sheet/70/db/var/siov_strap_ls40.pdf

[30] I. Kim, T. Funabashi, H. Sasaki, T. Hagiwara, and M. Kobayashi, "Study of ZnO arrester model for steep front wave," *IEEE Trans. Power Del.*, vol. 11, no. 2, pp. 834–841, Apr. 1996, doi: 10.1109/61.489341.

[31] W. Schmidt, J. Meppelink, B. Richter, K. Feser, L. E. Kehl, and D. Qui, "Behaviour of MO-surge-arrester blocks to fast transients," *IEEE Trans. Power Del.*, vol. 4, no. 1, pp. 292–300, Jan. 1989, doi: 10.1109/61.19216.

[32] W. Li, X. Yao, J. Sun, Q. Li, H. Wang, and X. Zhu, "Comparison with the influence of different types of impulse currents on the degradation of zinc-oxide varistors," in *Proc. IEEE Int. Conf. High Voltage Eng. Appl.*, 2020, pp. 1–4, doi: 10.1109/ICHVE49031.2020.9279444.

[33] D. T. Khanmiri, R. Ball, J. Mosesian, and B. Lehman, "Degradation of low voltage metal oxide varistors in power supplies," in *Proc. IEEE Appl. Power Electron. Conf. Expo.*, 2016, pp. 2122–2126, doi: 10.1109/APEC.2016.7468160.

[34] Y. Men, X. Lu, Z. Zhang, and R. Thiagarajan, "Metal oxide varistor (MOV) lifetime estimation with impulse-based testing in PV inverter systems," in *Proc. IEEE 13th Int. Symp. Power Electron. Distrib. Gener. Syst.*, 2022, pp. 1–4, doi: 10.1109/PEDG54999.2022.9923107.

[35] D. Van Niekerk and P. Bokoro, "Durability analysis of metal oxide varistor under direct current switching surges," in *Proc. Int. SAUPEC/RobMech/PRASA Conf.*, 2020, pp. 1–6, doi: 10.1109/SAUPEC/RobMech/PRASA48453.2020.9040958.

[36] X. Zhang, Z. Yu, Z. Chen, Y. Huang, B. Zhao, and R. Zeng, "Modular design methodology of DC breaker based on discrete metal oxide varistors with series power electronic devices for HVDC application," *IEEE Trans. Ind. Electron.*, vol. 66, no. 10, pp. 7653–7662, Oct. 2019, doi: 10.1109/TIE.2018.2886787.

[37] J. Magnusson, A. Bissal, G. Engdahl, R. Saers, Z. Zhang, and L. Liljestrand, "On the use of metal oxide varistors as a snubber circuit in solid-state breakers," in *Proc. IEEE PES ISGT Europe*, 2013, pp. 1–4, doi: 10.1109/ISGTEurope.2013.6695454.

[38] J. Magnusson, R. Saers, L. Liljestrand, and G. Engdahl, "Separation of the energy absorption and overvoltage protection in solid-state breakers by the use of parallel varistors," *IEEE Trans. Power Electron.*, vol. 29, no. 6, pp. 2715–2722, Jun. 2014, doi: 10.1109/TPEL.2013.2272857.

[39] X. Liao, H. Li, R. Yao, Z. Huang, and K. Wang, "Voltage overshoot suppression for SiC MOSFET-based DC solid-state circuit breaker," *IEEE Trans. Compon., Packag. Manuf. Technol.*, vol. 9, no. 4, pp. 649–660, Apr. 2019, doi: 10.1109/TCPMT.2019.2899340.

[40] F. Zhu, F. Liu, W. Liu, K. Feng, and X. Zha, "Performance analysis of RCD and MOV snubber circuits in low-voltage DC microgrid system," in *Proc. IEEE Appl. Power Electron. Conf. Expo.*, 2017, pp. 1518–1521, doi: 10.1109/APEC.2017.7930900.

[41] S. Zhao, R. Kheirollahi, H. Zhang, J. Wang, X. Lu, and F. Lu, "MOV-RCD snubber design for medium-voltage SiC-module based solid-state DC circuit breaker," in *Proc. IEEE 4th Int. Conf. DC Microgrids*, 2021, pp. 1–6, doi: 10.1109/ICDCM50975.2021.9504627.

[42] "Bourns 430V 6kA power TVS datasheet," Accessed: May 21, 204. [Online]. Available: https://www.bourns.com/docs/product-datasheets/ptvs6-xxxc-th_hv.pdf?sfvrsn=6a62e769_11

[43] K. Askan, M. Bartonek, and F. Stueckler, "Bidirectional switch based on silicon high voltage superjunction MOSFETs and TVS diode used in low voltage DC SSCB," in *Proc. PCIM Europe Int. Exhib. Conf. Power Electron., Intell. Motion, Renewable Energy Energy Manage.*, 2019, pp. 1–8.

[44] A. Fayyaz, M. U. Ortiz, Z. Wang, T. Yang, and P. Wheeler, "Paralleling of transient overvoltage protection elements within high power DC solid-state circuit breaker (SSCB) for electric/hybrid-electric aircraft," in *Proc. IEEE Workshop Wide Bandgap Power Devices Appl. Europe*, 2022, pp. 1–6, doi: 10.1109/WiPDAEurope55971.2022.9936092.

[45] M. F. Rahman, T. Pang, E. Shoubaki, N. Sakib, and M. Manjrekar, "Active voltage clamping of series connected 1.2kV SiC MOSFETs for solid state circuit breaker application," in *Proc. IEEE 7th Workshop Wide Bandgap Power Devices Appl.*, 2019, pp. 332–336, doi: 10.1109/WiPDA46397.2019.8998943.

[46] L. Rubino and G. Rubino, "Definition of the solid state circuit breaker limits working with active clamp driver," in *Proc. Int. Symp. Power Electron., Elect. Drives, Automat. Motion*, 2020, pp. 387–390, doi: 10.1109/SPEEDAM48782.2020.9161839.

[47] L. Rubino and G. Rubino, "On the active clamp gate driver thermal effects," in *Proc. Int. Conf. Clean Elect. Power*, 2019, pp. 478–481, doi: 10.1109/ICCEP.2019.8890213.

[48] J. G. Zola, "Gas discharge tube modeling with PSpice," *IEEE Trans. Electromagn. Compat.*, vol. 50, no. 4, pp. 1022–1025, Nov. 2008, doi: 10.1109/TEMC.2008.2004808.

[49] K. Liu, X. Zhang, L. Qi, X. Qu, and G. Tang, "A novel solid-state switch scheme with high voltage utilization efficiency by using modular gapped MOV for DC breakers," *IEEE Trans. Power Electron.*, vol. 37, no. 3, pp. 2502–2507, Mar. 2022, doi: 10.1109/TPEL.2021.3115254.

[50] W. A. Martin, C. Deng, D. Fiddiansyah, and J. C. Balda, "Investigation of low-voltage solid-state DC breaker configurations for DC microgrid applications," in *Proc. IEEE Int. Telecommun. Energy Conf.*, 2016, pp. 1–6, doi: 10.1109/INTLEC.2016.7749139.

[51] D. Li and A. Ukil, "Adaptive solid-state circuit breaker without varistors in VSC-interfaced DC system," *IEEE Trans. Ind. Electron.*, vol. 69, no. 5, pp. 4824–4835, May 2022, doi: 10.1109/TIE.2021.3080203.

[52] D. Park, D. Shin, S.-K. Sul, J. Sim, and Y.-G. Kim, "Overvoltage suppressing snubber circuit for solid state circuit breaker considering system inductances," in *Proc. 10th Int. Conf. Power Electron. ECCE Asia*, 2019, pp. 2647–2652, doi: 10.23919/ICPE2019-ECCEAsia42246.2019.8796957.

[53] W. Liu, H. Yang, F. Liu, J. Sun, and X. Zha, "An improved RCD snubber for solid-state circuit breaker protection against bus fault in low-voltage DC microgrid," in *Proc. IEEE 2nd Int. Future Energy Electron. Conf.*, 2015, pp. 1–5, doi: 10.1109/IFEEC.2015.7361508.
[54] G. Demetriades, W. Hermansson, and K. Papastergiou, "An arrangement for protecting a solid-state DC-breaker against transient voltages," Patent WO2011098145A1, 2011. [Online]. Available: https://patents.google.com/patent/WO2011098145A1/en
[55] R. Kheirollahi, S. Zhao, H. Zhang, and F. Lu, "Novel active snubbers for SSCBs to improve switch voltage utilization rate," *IEEE J. Emerg. Sel. Topics Power Electron.*, vol. 11, no. 3, pp. 2565–2576, Jun. 2023, doi: 10.1109/JESTPE.2022.3211459.
[56] T. Pang, M. F. Rahman, and M. D. Manjrekar, "A ground clamped solid-state circuit breaker for DC distribution systems," in *Proc. IEEE Energy Convers. Congr. Expo.*, 2020, pp. 989–994, doi: 10.1109/ECCE44975.2020.9235824.
[57] T. Pang and M. D. Manjrekar, "A surge voltage free solid-state circuit breaker with current limiting capability," in *Proc. IEEE Appl. Power Electron. Conf. Expo.*, 2021, pp. 389–394, doi: 10.1109/APEC42165.2021.9487057.
[58] R. Kheirollahi, S. Zhao, and F. Lu, "Fault current bypass-based LVDC solid-state circuit breakers," *IEEE Trans. Power Electron.*, vol. 37, no. 1, pp. 7–13, Jan. 2022, doi: 10.1109/TPEL.2021.3092695.
[59] T. Pang and M. D. Manjrekar, "A surgeless diode-clamped multilevel solid-state circuit breaker for medium-voltage DC distribution systems," *IEEE Trans. Ind. Electron.*, vol. 69, no. 7, pp. 7329–7339, Jul. 2022, doi: 10.1109/TIE.2021.3102419.
[60] L. Ravi, D. Zhang, D. Qin, Z. Zhang, Y. Xu, and D. Dong, "Electronic MOV-based voltage clamping circuit for DC solid-state circuit breaker applications," *IEEE Trans. Power Electron.*, vol. 37, no. 7, pp. 7561–7565, Jul. 2022, doi: 10.1109/TPEL.2022.3149757.

GIOELE GREGIS was born in Bergamo, Italy, in December 1997. He received M.Sc. degree *(cum laude)* in electrical engineering in 2021 from the Politecnico di Milano, Milan, Italy, where he has been working toward the executive Ph.D. degree in electrical engineer in collaboration with ABB, Bergamo, Italy, since 2021. He is currently a Power Electronics Engineer with the ABB, Bergamo, Italy. His research interests include power electronics, electrical machines and dc grids protection systems.

LUIGI PIEGARI (Senior Member, IEEE) was born in Naples, Italy, in April 1975. He received the M.S. *(cum laude)* and Ph.D. degrees in electrical engineering from the University of Naples Federico II, Naples, Italy, in 1999 and 2003, respectively.

From 2003 to 2008, he was a Postdoctoral Research Fellow with the Department of Electrical Engineering, University of Naples Federico II. From 2009 to 2012, he was an Assistant Professor with the Department of Electrical Engineering, Politecnico di Milano, Milan, Italy. From 2013 to 2023, he was an Associate Professor with the Department of Electrical Engineering, Politecnico di Milano, Milan, Italy, where he is currently a Full Professor of power electronics, electrical machines and drives with the Department of Electronics, Information and Bioengineering. He is the author of more than 150 scientific papers published in international journals and conference proceedings. His research interests include storage device modeling, wind and photovoltaic generation, modeling and control of multilevel converters, and dc distribution grids.

He is an Associate Editor for the IEEE JOURNAL OF EMERGING AND SELECTED TOPICS IN INDUSTRIAL ELECTRONICS and he was the General Co-Chair and Technical Program Chair for some IEEE sponsored and co-sponsored conferences. Prof. Piegari is also the Member of the IEEE Industrial Electronics Society, IEEE Power Electronics Society, IEEE Vehicular Technology Society, and AEIT.

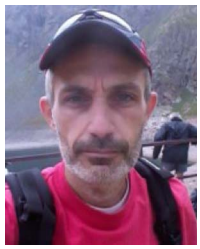

LUCA RACITI was born in Bergamo, Italy. He received the M.Sc. degree in electronic engineering from the Politecnico di Milano, Milan, Italy, in 1998. In 1998, he joined ABB, Bergamo, Italy, where he is currently Product Owner for power electronics with the Electrification Smart Power Division.

THOMAS MASPER was born in Bergamo, Italy, in October 1974. He received the M.Sc. degree in electronic engineering from the Politecnico di Milano, Milan, Italy, in 1999. In 2001, he joined ABB, Bergamo, Italy, where he is currently a Chapter Leader for power electronics for interruption and switching with the Electrification Smart Power Division.

Open Access funding provided by 'Politecnico di Milano' within the CRUI CARE Agreement